DUJASE Vol. 2(2) 85-89, 2014 (January)

Two-dimensional Electron Gas Mobility in AlN/InN Heterostructure at Low-temperature

M. Onirban Islam, Md. Raisul Islam and A.S.M. Moslehuddin

Department of Applied Physics, Electronics and Communication Engineering, University of Dhaka, Dhaka - 1000, Bangladesh

E-mail: m.onirbanislam@gmail.com

Received on 05. 07. 2012. Accepted for publication on 16.09. 2013.

Abstract

Two-dimensional electron gas (2DEG) mobility is studied for AlN/InN single heterostructure (SH) within the infinite potential well at low-temperature. The relaxation time approximation is used to solve the Boltzmann transport equation considering all possible scattering phenomena: background impurity, surface roughness, piezoelectric charge, and deformation potential. It is found that the screened and unscreened form factors for different scattering phenomena in AlN/InN diminishes at a slower rate with respect to wave number than those of well-studied AlGaN/GaN. The total mobility is calculated from the Matthiessen's rule. The form factors have been evaluated for different dimensionless parameter Λk. Variation of 2DEG mobility is studied for different roughness amplitude, correlation length, and background impurity density considering abrupt interface profile. The screening of scattering potential by the 2DEG has been implemented by the random phase approximation. The superiority of AlN/InN heterostructure over the conventional AlGaN/GaN heterostructure for high-speed device application is evident from the study

Keywords : Aluminium Nitride, Indium Nitride, Two-dimensional Electron Gas mobility.

1. INTRODUCTION

Heterostructure based transistors (HFETs), now a days have become devices of choice due to its high frequency response compared to other electronic devices. AlGaN/GaN HFETs are preferred over AlGaAs/GaAs due to high sheet charge density at the heterojunction which is around 10^{13}cm^2 [1]. 2DEG mobility is the key parameter for HFETs frequency response. Many theoretical as well as experimental studies have been done to calculate the mobility of 2D electron in AlGaN/GaN heterojunction. Three-dimensional approximation is considered by Shur *et al.* to find the mobility of these structures [2]. Hsu and Walukiewicz, by using variational principle calculation found that the optical phonon limits the room temperature mobility [3]. But they did not considered the polarization effect and surface roughness scattering phenomenon. Zhang *et al.* used Kubo formula to investigate electron transport in an AlGaN/GaN HFET [4]. Yu and Brennan calculated 2DEG mobility in III-nitdride heterostrcture using a self-consistent solution of the Schrödinger, Poisson, charge and potential balance equations considering polarization effect [6]. Monte Carlo simulation of the electron mobility in these structures has also been performed [7]. Quang *et al.* calculated the mobility in AlGaN/GaN structure accounting polarization effect and surface roughness scattering [10].

Recently, indium nitride(InN), a member of III-Nitride family, has become a promising material for manufacturing heterostructure due to its outstanding properties such as narrow band gap (0.65 eV), high electron saturation velocity (2.5×10^7cm/s^2), high bulk electron mobility (2250 cm^2/(Vs)), and low effective mass($0.07m_0$) [8]. Moreover, spontaneous and piezoelectric polarizations present in the wurtzite phase group-III nitride based heterojunction contribute to the polarization field and induces high 2DEG density in the order of 10^{14}cm^2 [9]. InN based heterojunnction exhibits higher sheet carrier concentration than GaN so there is a room for achieving higher mobility of 2DEG in InN based heterostructure.

2DEG mobility in AlN/InN at lowtemperature has been addressed in this article.

2. Low temperature Mobility

The theoretical investigation has been performed based on the single AlN/InN heterostructure fabricated by Fujii *et al.* [8]. Due to the lattice mismatch at the heterojunction, InN being channel material experiences piezoelectric effect as well as the characteristic spontaneous polarization of III-Nitrides. Consequently, the strained state at AlN/InN SH significantly affects the band profile and electromechanical coupling constants. Fang-Howard wave function is used for the infinite quantum well considering all possible scattering phenomena. It has been found that the mobility increases as a function of sheet carrier concentration.

2.1 Basic theory

Calculation of the low-temperature mobility has been done using the mathematical formulation developed by Quang *et al.*

[10, 11]. The multiple scattering effects are negligibly small for high sheet density ($n_s \geq 10^{12} cm^{-2}$). It is evident that all III-N SHs exhibit bound charges as well as high sheet carrier density. Therefore the linear transport theory is used as a good approximation. The inverse transport relaxation time for zero-temperature is expressed in terms of the autocorrelation function of disorder

$$\tau = \frac{1}{2\pi\hbar E_F}\int_0^{2k_F} dq \frac{q^2}{\sqrt{4k_F^2 - q^2}} \frac{\langle |U(q)|^2 \rangle}{\varepsilon^2(q)} \quad (1)$$

where q = (q, θ) denotes a 2D wave vector in the xy plane given in polar coordinates, representing the momentum transfer by a scattering event in the inerface plane $q = |q| = 2k_F \sin(\theta/2)$, θ as an angle of scattering. The Fermi energy and the Fermi wave vector are, $E_F = \sqrt{(\hbar^2/2m_z^*)k_F^2}\, k_F = \sqrt{2m_z^*(E_F - E_0)}/\hbar$ respectively. By using the Fang-Howard wave function y(z) [10, 12] the 2D Fourier transform of the unscreened potential for the lowest subband wave function can be written as,

$$U(q) = \int_{-\infty}^{\infty} dz |\psi(z)|^2 U(q,z) \quad (2)$$

The dielectric function ε(q) in Eq. (1) gives the screening of the scattering potentials by the 2DEG/2DHG and it is treated as the random phase approximation (RPA) [12]

$$\varepsilon(q) = 1 + \frac{q_{TF}}{q} F_S(t)[1 - G(t)] \quad (3)$$

Where, q_{TF} is the inverse 2D Thomas-Fermi screening length:

$$q_{TF} = \frac{2m_z^* e^2}{\varepsilon(0)\varepsilon_L \hbar^2} \quad (4)$$

m_z^* is the band effective-mass tensor along the growth direction, e is the electronic charge, $\hbar$ is the reduced Planck's constant, ε(0) is the static permittivity of vacuum and the dielectric constant ε_L is given by

$$\varepsilon_L = \frac{\varepsilon(0)_{epi} + \varepsilon(0)_{InN}}{2} \quad (5)$$

The screening form factor $F_S(t)$ depends on the electron distribution, i.e., the envelop wave function ψ(z). For limiting case of infinitely deep QWs [12]

$$F_s(t) = \frac{3t^2 + 9t + 8}{8(t+1)^3} \quad (6)$$

with t ≡ q/k as the dimensionless in-plane wave vector and k is the quantum well wave vector given by

$$k = \sqrt{\frac{48\pi m_z^* e^2}{\hbar^2 \varepsilon_o \varepsilon_L}\left[\frac{11 n_s}{32} + \frac{\sigma}{2e} - N_I z_\omega\right]} \quad (7)$$

The many-body exchange effect in the in-plane is given by the form factor

$$G(t) = \frac{t}{2(t^2 + t_F^2)}; \quad t_F \equiv \frac{k_F}{k} \quad (8)$$

The total relaxation time is determined by using the Matthiessen's rule

$$\frac{1}{\tau} = \frac{1}{\tau_{BI}} + \frac{1}{\tau_{SR}} + \frac{1}{\tau_{PE}} + \frac{1}{\tau_{DP}} \quad (9)$$

2.2 Scattering mechanism

The scattering mechanisms studied for the InN based SH have been assumed to be the same as those for wurtzite phase AlGaN/GaN SH due to the same crystal symmetry group. The necessary mathematical equations for all possible scattering phenomena are briefly summarized as follows.

2.2.1 Background Impurity (BI)

Infinitely deep triangular QW is a good approximation for the special case of uniform doping, where the 2DEG is surrounded by the impurities. The study was done considering the doping regions in the well and barrier layers to be infinitely long. Moreover, the sample is subjected to thermal treatment during epitaxial growth process; therefore high-temperature ionic correlation has to be considered. Due to the diffusion Coulomb interaction between the charge impurities diminish and thereby there will not be any large density fluctuations which implies that large ionic correlation weakens the impurity scattering.

The 2D Fourier transform of autocorrelation function of background doping of the whole sample can be given as [10], [11]

$$\langle |U_{BI}(q)|^2 \rangle_c = \left(\frac{2\pi e^2}{\varepsilon_L}\right)^2 \frac{N_I}{2k^3} F_{BI}^{uns}\left(\frac{q}{k}\right) \quad (10)$$

where $\langle ... \rangle_c$ stands for the averaging over a correlated impurity distribution and the form factor is defined by

$$F_{BI}^{uns}(t) \equiv \frac{1}{t^2(t+t_c)}[d_1(t) - 12d_2(t) - 4d_3(t) + 6d_4(t) + d_5(t) - d_5(-t)] \quad (11)$$

provided,

$$d_1(t) = \frac{1}{(t-1)^6} \quad (12)$$

$$d_2(t) = \frac{t}{(t+1)^4(t-1)^3} \quad (13)$$

$$d_3(t) = \frac{t}{(t+1)^2(t-1)^6}\left[2 + \frac{(t-1)^2}{(t+1)}\right] \quad (14)$$

$$d_4(t)=\frac{t}{(t^2-1)^3}\left[1-\frac{t^2-1}{4}+\frac{(t^2-1)^2}{8}\right] \quad (15)$$

$$d_5(t)=\frac{t}{(t+1)^6}\left[2+t+(t+1)^2+\frac{3(t+1)^3}{4}+\frac{3(t+1)^4}{8}\right]$$

and the dimensionless parameter t_c which quantifies the ionic correlation effect is given by

$$t_c=\frac{2\pi e^2 n_I}{\varepsilon_L k_B T_0}\frac{1}{k} \quad (16)$$

Where, T_0 is the freezing temperature for impurity diffusion (~1000 K) and nI is the sheet impurity density, given by $n_I = N_I^{2/3}$

2.2.2 Surface Roughness (SR)

In the wave vector space the weighted scattering potential is fixed by the value of the envelop wave function y at the interface plane. For infinite deep QWs [10]:

$$\langle |U_{SR}(q)|^2\rangle = \left[\frac{4\pi e^2}{\varepsilon_L}\right]^2\left[\frac{n_s}{2}+\frac{\sigma}{2e}-N_I z_\varpi\right]^2\langle|\Delta_q|^2\rangle \quad (17)$$

Where, the Fourier transform of the interface roughness profile is given by

$$\left\langle|\Delta_q|^2\right\rangle = \pi\Delta^2\Lambda F_{SR}^{uns}(q/k) \quad (18)$$

Where, Δ is the roughness amplitude and Λ is the correlation length. The unscreened form factor for surface roughness is given by

$$F_{SR}^{uns} = \frac{1}{\left[1+(\Lambda k)^2/4n\right]^{n+1}} \quad (19)$$

Where, n is an exponent fixing the falloff of the distribution at large in-plane wave numbers. In this work, smooth surface profile has been used, i.e., n = 4, and Λ is the fitting parameter.

2.2.3 Misfit Piezoelectric Charges (PE)

Surface roughness due to lattice mismatched at the epitaxial layer gives rise to strain fluctuations in both strained and relaxed layers [13, 14]. Wurtzite nitride heterostructures, e.g., in AlGaN/GaN, AlN/InN, these induce fluctuating densities of piezoelectric charges, viz. bulk charges inside the strained and relaxed layers as well as sheet charges at the interface [13]. The charges create random electric fields and act as scattering sources on the motion of electrons in the in-plane [11]. The effect on the 2DEG of the piezoelectric field due to charges in the well has been found much stronger than the charges in the barrier and the interface [13]. Therefore, the calculation for the scattering by charges inside the well has only been considered. Using the lowest subband wave function $\psi(z)$, the 2D Fourier transform of the autocorrelation function for roughness-induced misfit piezoelectric charge is given by [11, 10]

$$\langle|U_{PE}(q)|^2\rangle = \left[\frac{\pi^{3/2}\alpha\epsilon_{AlN/InN}eQ\Delta\Lambda}{\varepsilon_L}\right]^2 F_{PE}^{uns}\left(\frac{q}{k}\right) \quad (20)$$

where α denotes the anisotropy ratio as a measure of the deviation of hexagonal symmetry of wurtzite crystal from isotropy (α ~ 5), the inplane Basel strain of the InN layer is defined as $\epsilon_{AlN/InN}(x) \equiv (a_{sub(buf)} - a(x))/a(x)$, and Q is a material parameter characteristic of the well, defined as

$$Q=\frac{C_B}{C_{33}^b}\left[\frac{e_{15}^W}{C_{44}^W}+\frac{e_{31}^W(C_{33}^W+2C_{13}^W)-e_{33}^W(C_{11}^W+C_{12}^W+C_{13}^W)}{C_W}\right] \quad (21)$$

where ι = W, B as the labels for the well and barrier layers, respectively, and

$$C_\iota = C_{33}^\iota(C_{11}^\iota + C_{12}^\iota) - 2(C_{13}^\iota)^2, \quad (22)$$

The form factor for infinite potential barrier becomes

$$F_{PE}^{uns}(t)=\frac{F_{SR}^{uns}(t)}{(t+1)^6}\left(\frac{3t}{t+1}+\frac{1}{2}\right)^2. \quad (23)$$

2.2.4 Misfit deformation potential (DP)

Strain fluctuation induces no uniform shifts of band edges which implies that electrons in the conduction band and holes in the valence band must experience a random perturbation potential. The roughness-induced misfit deformation potentials exists both in the well and the barrier and decay exponentially far away from the interface. As 2DEG is located very close to the interface, only the scattering in this layer has been taken into account. Using the wave function y(z), the 2DFourier transform of the autocorrelation function can be given by [10]

$$\langle|U_{DP}(q)|^2\rangle = \left[\frac{\sqrt{\pi}\alpha\epsilon_{AlN/InN}\Xi_d\Delta\Lambda}{2}\frac{C_B}{C_{33}^B}\frac{C_{11}^W+C_{12}^W+C_{13}^W}{C_W}\right]^2\times k^2F_{DP}^{uns}\left(\frac{q}{k}\right) \quad (24)$$

where Ξ_d is the combined dilational component of the deformation potential for the conduction band, and the form factor for the infinitely deep QW is

$$F_{DP}^{uns}(t)=\frac{F_{SR}^{uns}(t)}{2}\frac{t^2}{(t+1)^4} \quad (25)$$

3. Result and Discussion

The form factors for all possible scattering events at low-temperature have been shown in Fig. 1 for different values of Λk, from which the total low-temperature 2DEG mobility is obtained and is shown in Fig. 2 for different sheet carrier concentration.

The unscreened form factors for background impurity (BI), surface-roughness (SR), misfit piezoelectric charges (PE), and misfit deformation potential (DP) are given by Eqs. (11, 20, 24, and 26) respectively. The screened form factors governed by Eq. (6) have also been shown. The screening of scattering potentials have been calculated under the random phase approximation of the dielectric function ε(q) using Eq. (3).

The local field correlations associated with the many-body interaction in 2DEG has been accounted by the function G(q), given by Eq. (8). The screening length is defined by the Thomas-Fermi wave vector q_{TF} , Eq. (4). Fermi wave vector has been chosen as the cutoff length of momentum transfer

The Fig. 1 reveals the fact that the form factors diminish in relatively larger wave number in InN than GaN [10]. In all cases, form factors reduce with increasing correlation length Λ.

2DEG is shown in Figs. 2 for different combination of fitting parameters, Λ, Δ, and background impurity N_I.

It is quite evident from Fig. 2, that 2DEG mobility in the AlN/InN heterostructure is about 10 times higher than that of AlGaN/GaN [11]. Also, the increase in mobility with sheet carrier concentration is much higher in InN than GaN. This clearly reveals the superiority of AlN/InN heterostructure over AlN/GaN for high-frequency applications.

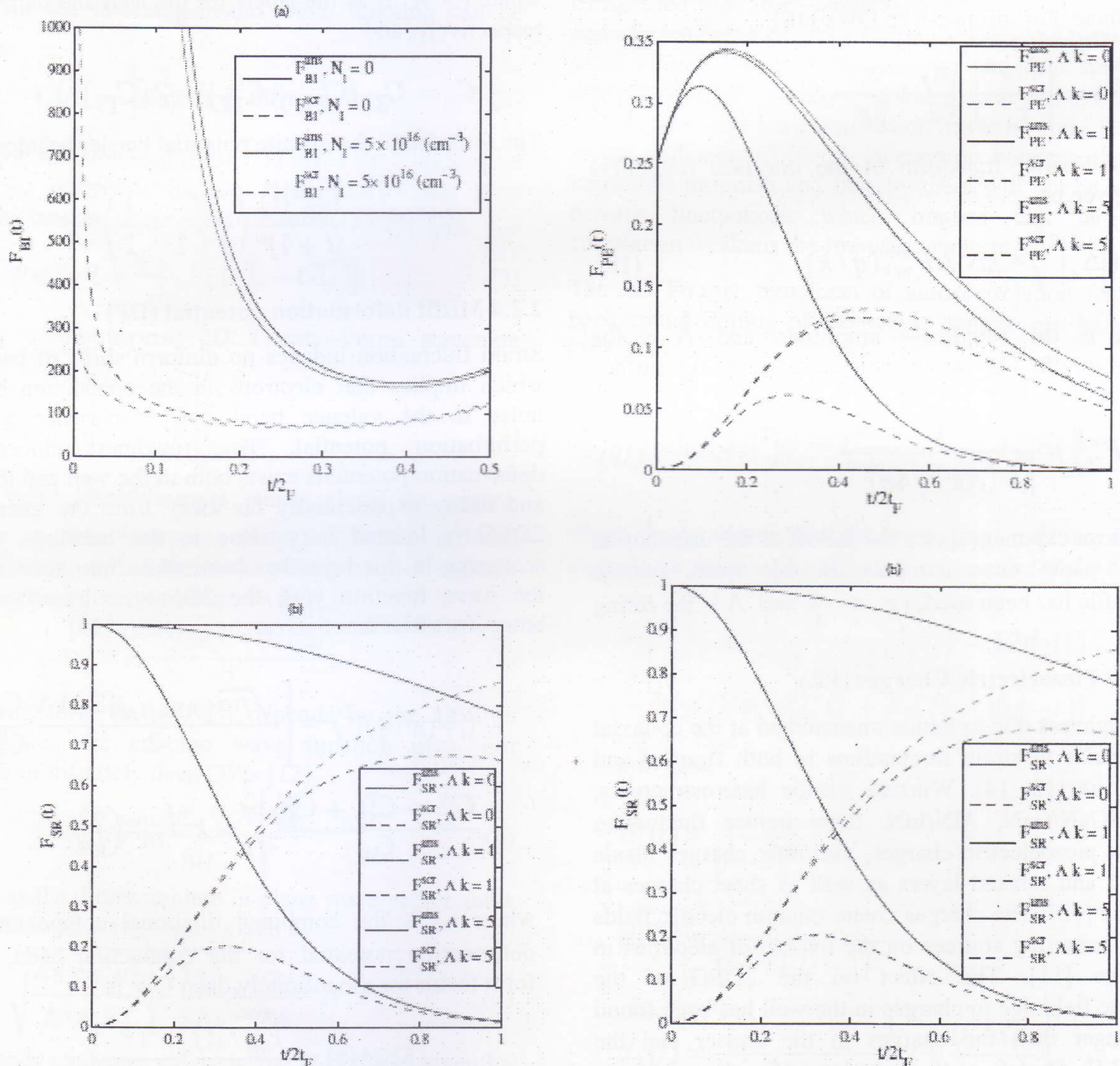

Fig. 1: Screened $F^{scr}(t)$ and unscreened $F^{uns}(t)$ form factors variation with dimensionless momentum transfer t in units of 2tF for (a) background impurity, (b) surface-roughness, (c) misfit piezoelectric charge, and (d) misfit deformation potential.

The individual motility for different scatterings are also much higher in InN than in GaN. The combined dilation component of the deformation potential for InN has been calculated from the expression mentioned in [15]. The mobility due to only misfit piezoelectric charge is almost 1000 times higher than that of AlN/GaN [11]. The physical origin behind this behavior is the much greater strain in AlN/InN than in AlN/GaN; ϵ(AlN/InN) ~ 1.4 where ϵ(AlN/GaN) ~ 0.025, gives ϵ^2(AlN/InN) much greater than ϵ^2 (AlN/GaN).

4. Conclusions

In this article, we have presented the 2DEG low-field mobility at low-temperature for AlN/InN heterostructure. The calculated result shows the mobility of 2DEG is in the o.der of $10^4 cm^2/Vs$. This simulated result is then also compared with the GaN-based hetrostructure. All individual scattering phenomena limited mobility in InN-based heterostructure have been found 10 times greater than that of GaN-based heterostructure. The theoretical results clearly indicate the high-potentiality of InN-based hetereostructures for high frequency applications.

In future, the authors are interested to investigate the room-temperature behavior of InN-based heterostrcture considering both the conventional and possible novel scattering phenomena for finite potential barrier. Beyond the RPA and the envelop function approximation are also e.xpected.

References

1. Mishra, U.K. and J. Singh, 2008 "Semiconductor Device Physics and Design", The Netherlands: Springer, p 378.
2. Shur, M., B. Gelmont, and M. Asif Khan, 1996, "High Electron mobility in twodimensional and in bulk GaN," J. Electron. Mater. 25, 777.
3. Hsu, L. and W. Walukiewicz, 1997, "Electron mobility in AlxGa1??xN/GaN heterostructures," Phys. Rev. B 56, 1520.
4. Zhang, Y. and J. Singh, 1999, "Charge control and mobility studies for an AlGaN/GaN high electron mobility transistor," J. Appl. Phys. 85, 587.
5. Ridley, B.K., B.E. Foutz, and L.F. Eastman, 2000, "Mobility of electrons in bulk GaN and $Al_xGa_{1-x}N$/GaN heterostructures," Phys. Rev. B 61, 16862.
6. Yu, T.H. and K.F. Brennan, 2001, "Theoretical study of the two-dimensional electron mobility in strained III-nitride heterostructures," J. Appl. Phys. 89, 3827 .
7. Polyakov, V. M., F. Schwierz, I. Cimalla, M. Kittler, B. L¨ ubbers, and A. Schober, 2009, "Intrinsically limited mobility of the two-dimensional electron gas in gated AlGaN/GaN and AlGaN/AlN/GaN heterostructures," J. Appl. Phys. 106, 023715.
8. Fujii, T., K. Shimomoto, R. Ohba, Y. Toyoshima, K. Horiba, J. Ohta, H. Fujioka, M. Oshima, S. Ueda, H. Yoshikawa, and K. Kobayashi, 2009, "Fabrication and Characterization of AlN/InN Heterostructures," Appl. Phys. Exp. 2, 011002.
9. Uddin, M.A., T.N. Upal, M.R. Islam, M.O. Islam, and Z.H. Mahmood, 2009 "Study of 2DEG at $In_xGa_{1-x}N$/InN and GaN/InN heterointerface," in Proc. 15th Int.Workshop on the Physics of Semiocnductor Devices (IWPSD), (New Delhi, India: December 14 - 19, 2009), pp. 655 - 658.
10. Qunag, D.N., N.H. Tung, V.N. Tuoc, N.V. Minh, H.A. Huy, and D.T. Hien, 2006, "Quantum and transport lifetimes due to roughness-induced scattering of two dimensional electron gas in wurtzite group- III-nitride heterostructures," Phys. Rev. B 74, 205312.
11. Quang, D.N., V.N. Tuoc, N.H. Tung, N.V. Minh, and P.N. Phong, 2005, "Roughness induced mechanisms for electron scattering in wurtzite group-III-nitride heterostructures," Phys. Rev. B 72, 245303.
12. Ando, T., A.B. Fowler, and F. Stern, 1982, "Electronic properties of two-dimensioanl systems", Rev. Mod. Phys. 54, 437.
13. Quang, D.N., N.H. Tung, V.N. Tuoc, T.D. Huan, and P.N. Phong, 2005, "Roughnessinduced piezoelectric charges in wurtzite group-III-nitride heterostrcture," Phys. Rev. B 72, 115337.
14. Quang, D.N., V. N. Tuoc, N. H. Tung, and T. D. Huan, 2002, "Random piezoelectric field in real [001]-oriented strain-relaxed semiconductor heterostrcture," Phys. Rev. Lett. 89, 077601.
15. Ghosh, S., P. Waltereit, O. Brandt, H.T. Grahn, and K.H. Ploog, 2002, "Electronic band structure of wurtzite GaN under biaxial strain in th eM plane investigated with photoreflectance spectroscopy," Phys. Rev. B 65, 075202.7